Driven Reconnection in Magnetic Fusion Experiments

Richard Fitzpatrick

Institute for Fusion Studies & Department of Physics,
The University of Texas at Austin,
Austin, Texas 78712

Lecture Given at Summer School
on
"MHD Phenomena in Plasmas"
held in
Madison, Wisconsin, 14-18 August 1995

Abstract

Error fields (i.e. small non-axisymmetric perturbations of the magnetic field due to coil misalignments, etc.) are a fact of life in magnetic fusion experiments. What effects do error fields have on plasma confinement? How can any detrimental effects be alleviated? These, and other, questions are explored in detail in this lecture using simple resistive magnetohydrodynamical (resistive MHD) arguments. Although the lecture concentrates on one particular type of magnetic fusion device, namely, the tokamak, the analysis is fairly general and could also be used to examine the effects of error fields on other types of device (e.g. Reversed Field Pinches, Stellerators, etc.).
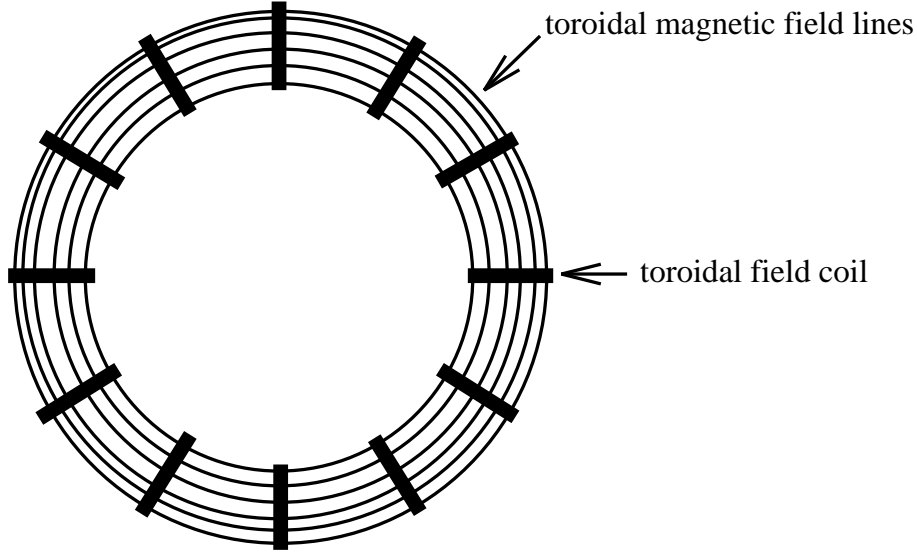
Figure 1: Schematic top view of a tokamak showing the toroidal magnetic field and its generating field coils

1   Introduction

Thermonuclear fusion requires plasma temperatures in excess of 10 keV (about 10^8 degrees kelvin). Obviously, this precludes containment of the plasma by solid walls. A "tokamak" is designed to confine a thermonuclear plasma on a set of nested toroidal magnetic flux surfaces. The magnetic field strength must be sufficiently high (i.e. $B \gtrsim 1$ tesla) that the Lamor radii of 3.5 MeV fusion product alpha particles are small compared to the dimensions of the device. The dominant magnetic field in a tokamak is toroidal and is generated by poloidal currents flowing around a set of (24 is a typical number) equally spaced field coils (see Fig. 1).

A toroidal magnetic field cannot by itself confine a plasma. Confinement is only possible if field lines rotate helically as they flow around the device in the toroidal direction. Thus, if a field line is chosen at random and followed for very many toroidal transits it ought to map out a closed toroidal *surface* (a pure toroidal field would only map out a closed toroidal *line*). Field lines in tokamaks are made to rotate helically via a comparatively small poloidal magnetic field
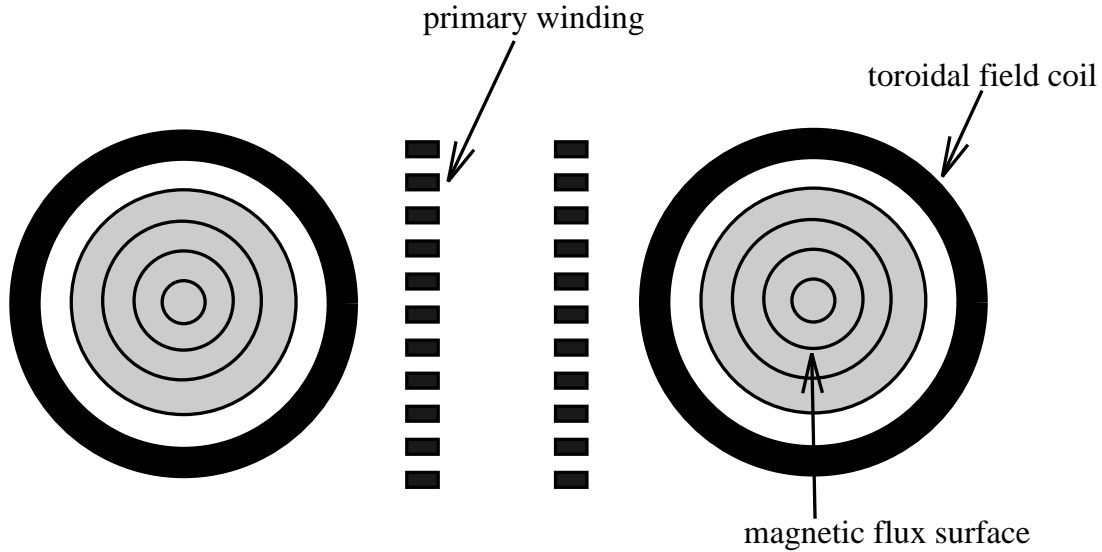
Figure 2: Schematic poloidal cross section of a tokamak showing the primary winding

which is induced by a toroidal current flowing through the plasma itself. The toroidal plasma current (which is typically a few mega-amps) is produced by transformer action. The plasma acts as a single turn secondary winding which is energized by the changing magnetic flux generated by a multi-turn primary winding situated in the centre of the torus (see Fig. 2).

A set of toroidal field coils, a primary winding, and a hot conducting plasma are sufficient to produce a set of toroidal magnetic flux surfaces. However, there is no guarantee that the plasma confined on these surfaces is in force balance. In fact, a toroidal plasma has a natural tendency to expand outward to ever larger major radius. In tokamaks this tendency is counteracted by an inward force due to the cross product of the plasma current with a "vertical" magnetic field produced by two poloidal coils situated above and below the plane of the torus. A judicious choice of the current which flows in these coils can maintain the plasma in force balance at a given major radius (see Fig. 3).

A basic tokamak can be built using a set of toroidal field coils, a primary winding, and a pair of vertical field coils. However, modern tokamaks are generally more complicated than this. For a given toroidal magnetic field strength
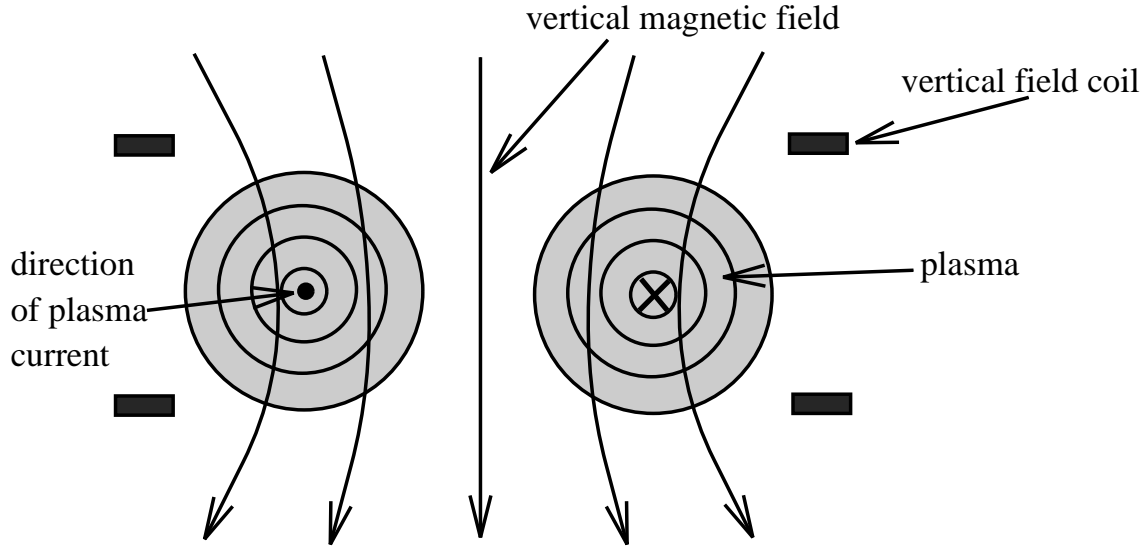
Figure 3: Schematic poloidal cross section of a tokamak showing the vertical field coils

the toroidal current which flows through the plasma is limited by magnetohydodynamical (MHD) stability considerations. This limit (the so-called Shafranov limit) is alleviated somewhat if the plasma flux surfaces are vertically elongated. Thus, a plasma with flux surfaces of elliptical cross section can carry more current than one with flux surfaces of circular cross section. Since plasma performance increases with increasing plasma current it is generally considered desirable to elongate the flux surfaces. Unfortunately, elongated plasmas are unstable to rigid shifts in the vertical direction. The ability of the vertical field coil system to feedback stabilize these modes sets a limit on how elongated the plasma can become. Plasmas whose flux surface cross sections are somewhat triangular tend to be more stable to MHD instabilities than non-triangular plasmas. Triangular flux surfaces also reduce the electromagnetic stresses acting on the toroidal field coils. Plasmas can be made elongated and triangular by using additional pairs of poloidal field coils to push and pull the equilibrium at various different poloidal locations (see Fig. 4).

It is clear that very many magnetic field coils are required to support the plasma equilibrium of a modern tokamak. Ideally, all of these coils are perfectly aligned, so that they generate a toroidally symmetric magnetic field (apart from
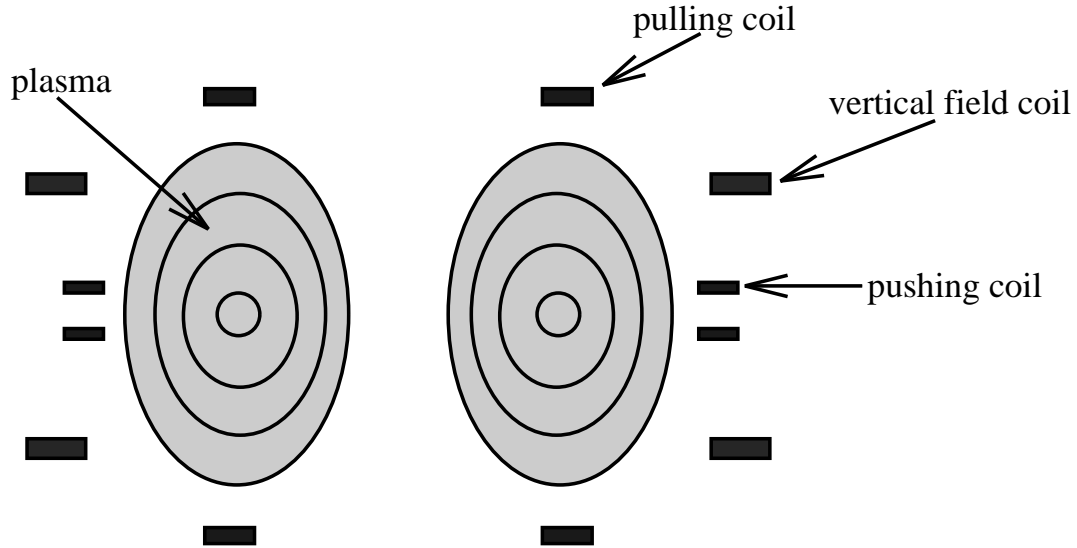
Figure 4: Schematic poloidal cross section of a tokamak show how two pairs of shaping coils can be used to produce plasma elongation

the inevitable ripple in the toroidal field due to the finite number of toroidal field coils: this effect is negligible provided there are sufficient (i.e. $18+$) coils). In practice, perfectly alignment of the coils is impossible to achieve. Coils are often slightly shifted from their proper positions; they can also be tilted, or they can even be not quite circular. A set of slightly misaligned field coils generate the required nested toroidal flux surfaces *plus* a low amplitude helical magnetic perturbation. This perturbation is known as the "error field". The leads which feed current to and from the field coils can also contribute to the error field if they are not properly designed. The error field is conventionally specified in terms of its Fourier amplitudes in the toroidal (ϕ) and poloidal (θ) angles around the tokamak. In present day tokamaks the low mode number Fourier amplitudes of the error field inside the plasma are typically a few gauss (i.e. about 10^{-4} of the equilibrium toroidal magnetic field strength). It is difficult to envisage building a tokamak with a significantly smaller error field than this because it is impossible to position field coils to an accuracy of much less than a few milli-meters in a device whose dimensions are a few tens of meters. Since error fields are clearly unavoidable in tokamaks it is important to understand what effects they have on the confinement properties of the equilibrium magnetic flux surfaces.

2 Phasing in Induction Motors

2.1 Introduction

The physics which governs the response of a tokamak plasma to an error field is very similar to that which governs the behaviour of a conventional induction motor. Consider a very simple induction motor consisting of a freely rotating, thin, hollow, cylindrical, conducting shaft surrounded by a set of rotating magnetic field coils. The idea of an induction motor is that the eddy currents induced in the shaft, crossed with the magnetic field due to the rotating coils, force the shaft to (almost) co-rotate with the coils. In a real motor the rotating shaft is used to drive machinery. In Fig. 5 the load on the motor is conveniently represented as a viscous coupling to a stationary non-conducting core.

2.2 Preliminary Analysis

Conventional cylindrical polar coordinates (r, θ, z) are adopted in the following analysis. The system is assumed to be symmetric in the z-direction. The magnetic field can be written in terms of a flux function,

$$\delta \mathbf{B} = \nabla \psi \wedge \hat{\mathbf{z}}, \tag{1}$$

where

$$\mu_0 \, \delta \mathbf{j} = \nabla \wedge \delta \mathbf{B} = -\nabla^2 \psi \, \hat{\mathbf{z}}. \tag{2}$$

For the sake of simplicity, the magnetic field is assumed to be dominated by a single Fourier harmonic in the angle θ, so that

$$\psi(r, \theta) = \psi(r) \, \exp(\mathrm{i} \, (m \, \theta - \omega_c \, t)), \tag{3}$$

where ω_c is the constant angular "rotation" frequency of the coils.[1] In the example shown in Fig. 5 the field is likely to be dominated by the $m = 6$ harmonic. The, as yet undetermined, angular "rotation" frequency of the shaft is denoted ω_{w}. The

---

[1] Actually, it is the angular rotation frequency divided by m.

"slip frequency", $\omega \equiv \omega_{\mathrm{w}} - \omega_c$, is the difference in "rotation" frequency between the shaft and the coils. It is helpful to define the "time constant" of the shaft,

$$\tau_{\mathrm{w}} = \mu_0\,\sigma_{\mathrm{w}} r_{\mathrm{w}} \delta_{\mathrm{w}}, \tag{4}$$

where σ_{w}, r_{w}, and δ_{w} are the shaft conductivity, radius, and thickness, respectively. The radial extent of the shaft is from $r = r_{\mathrm{w}} - \delta_{\mathrm{w}}$ to $r = r_{\mathrm{w}}$. In the "thin shell" limit, which corresponds to

$$\frac{\delta_{\mathrm{w}}}{r_{\mathrm{w}}} \ll |\omega|\tau_{\mathrm{w}} \ll \frac{r_{\mathrm{w}}}{\delta_{\mathrm{w}}}, \tag{5}$$

the skin depth in the material which makes up the shaft is much less than its radius but much greater than its thickness. In this regime there is negligible radial variation of the magnetic flux function $\psi(r)$ across the shaft. In addition, Ohm's law and Faraday's law integrated across the shaft yield

$$\left[r\,\frac{d\psi}{dr} \right]_{r_{\mathrm{w}}-\delta_{\mathrm{w}}}^{r_{\mathrm{w}}} = \mathrm{i}\,\omega\tau_{\mathrm{w}}\,\Psi_{\mathrm{w}}, \tag{6}$$

where $\Psi_{\mathrm{w}} \equiv \psi(r_{\mathrm{w}})$ is the magnetic flux which penetrates into the shaft.

Outside the shell there are no currents, so $\nabla^2\psi = 0$. The most general solution is

$$\psi(r) = \Psi_{\mathrm{w}} \left(\frac{r}{r_{\mathrm{w}}} \right)^m \tag{7}$$

for $r < r_{\mathrm{w}} - \delta_{\mathrm{w}}$, and

$$\psi(r) = \Psi_v \left(\frac{r}{r_{\mathrm{w}}} \right)^m + (\Psi_{\mathrm{w}} - \Psi_v) \left(\frac{r}{r_{\mathrm{w}}} \right)^{-m} \tag{8}$$

for $r_{\mathrm{w}} < r < r_c$, where r_c is the radius of the rotating field coils. It is convenient to parameterize the amplitude of the magnetic field generated by the coils in terms of Ψ_v, the flux which would penetrate into the shaft in the absence of any induced eddy currents. Equations (6)–(8) yield

$$\Psi_{\mathrm{w}} = \frac{\Psi_v}{1 + \mathrm{i}\,\omega\tau_{\mathrm{w}}/2m}. \tag{9}$$
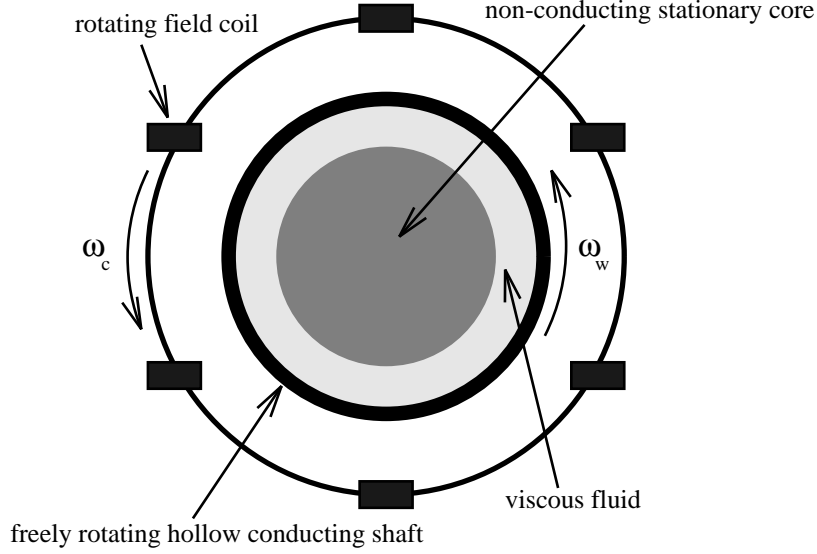
Figure 5: Schematic diagram of a simple induction motor

According to the above relation, if the slip frequency is much less than $2m/\tau_{\rm w}$ then the eddy currents induced in the shaft are weak and the flux $|\Psi_{\rm w}|$ which penetrates into the shaft attains its maximum amplitude $|\Psi_v|$. However, if the slip frequency is much greater than $2m/\tau_{\rm w}$ then the eddy currents induced by the relative rotation of the shaft and the field coils are strong enough to exclude magnetic flux from the shaft, so that $|\Psi_{\rm w}| \ll |\Psi_v|$.

2.3   Electromagnetic Torques

The integrated electromagnetic torque per unit length acting on the shaft is given by

$$T_{\theta\,\rm EM} = \int_{r_{\rm w}-\delta_{\rm w}}^{r_{\rm w}} \oint r\,\delta j_z\,\delta B_r\;rd\theta\,dr = -\frac{\pi m}{\mu_0}\,{\rm Im}\left(\left[r\,\frac{d\psi}{dr} \right]_{r_{\rm w}-\delta_{\rm w}}^{r_{\rm w}}\;\Psi_{\rm w}^{\,*} \right). \qquad (10)$$

Equations (6) and (9) yield

$$T_{\theta\,\rm EM} = -\frac{\pi m^2\,|\Psi_v|^2}{\mu_0}\,\frac{2\,(\omega\tau_{\rm w}/2m)}{1+(\omega\tau_{\rm w}/2m)^2}. \qquad (11)$$
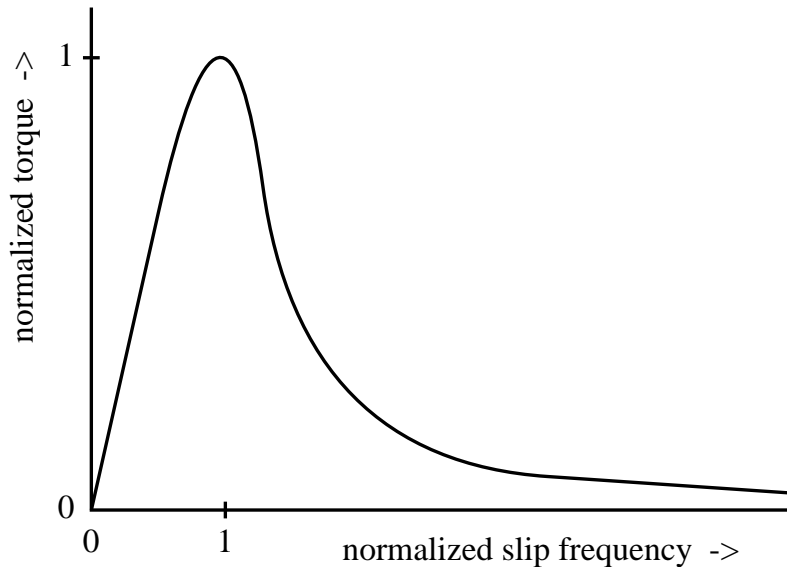
8

Figure 6: Schematic graph of the variation of the normalized electromagnetic torque, $T_{\theta\,\mathrm{EM}}/(-\pi m^2\,|\Psi_v|^2/\mu_0)$, with the normalized slip frequency, $\omega\tau_\mathrm{w}/2m$

The electromagnetic torque always acts to reduce the slip frequency and thereby make the shaft rotate with the coils. The torque has a very characteristic *non-monotonic* variation with the slip frequency (see Fig. 6). If the slip frequency is zero (i.e. if the shaft co-rotates exactly with the coils) then there is zero torque because no eddy currents are induced in the shaft. The torque initially increases *linearly* with the slip frequency because the eddy current strength per unit magnetic flux scales linearly with the slip frequency. However, as the slip frequency approaches the critical value $2m/\tau_\mathrm{w}$ the eddy currents start to exclude magnetic flux from the shaft and the rate of increase of the torque begins to level off (because there is less magnetic field in the shaft to cross with the eddy currents and thereby produce a torque). The torque attains its maximum value, $-\pi m^2|\Psi_v|^2/\mu_0$, at the critical frequency. For slip frequencies higher than the critical frequency the exclusion of magnetic flux from the shaft becomes more complete and the torque starts to decrease with increasing slip frequency. At slip frequencies much higher than the critical value the torque is *inversely proportional* to the slip frequency.

9

2.4 Torque Balance

The rotation of the shaft is transmitted to the viscous fluid (see Fig. 5), which exerts a slowing down torque on the shaft. Suppose that the spacing, d, between the inside of the shaft and the non-rotating core is much less than the radius of the shaft. In this limit, the viscous torque per unit length acting on the shaft is

$$T_{\theta\,\mathrm{VS}} \simeq -\frac{2\pi\mu r_{\mathrm{w}}^3}{md}\,\omega_{\mathrm{w}}, \tag{12}$$

where μ is the coefficient of viscosity of the fluid.

In steady-state the electromagnetic and viscous torques acting on the shaft must balance, so

$$T_{\theta\,\mathrm{EM}} + T_{\theta\,\mathrm{VS}} = 0. \tag{13}$$

The torque balance equation can be written

$$\frac{m^2\tau_{\mathrm{w}}d\,|\Psi_v|^2}{2\mu_0\mu r_{\mathrm{w}}^3}\frac{\omega}{1+(\omega\tau_{\mathrm{w}}/2m)^2} = |\omega_c| - \omega, \tag{14}$$

where the coil "rotation" frequency ω_c is taken to be negative for convenience (this ensures that the slip frequency is always positive). It is easily demonstrated that there is a critical "rotation" frequency of the coils,

$$(\omega_c)_{\mathrm{crit}} = \frac{6\sqrt{3}\,m}{\tau_{\mathrm{w}}}. \tag{15}$$

If the magnitude of the coil "rotation" frequency is much less than the critical value then the slip frequency never gets sufficiently large to exclude magnetic flux from the shaft and the variation of the slip frequency with the coil field strength is consequently quite smooth, i.e.

$$\omega \simeq \frac{|\omega_c|}{1+|\Psi_v|^2/|\Psi_{v1}|^2}, \tag{16}$$

where

$$\Psi_{v1} = \sqrt{\frac{2\mu_0\mu r_{\mathrm{w}}^3}{m^2\tau_{\mathrm{w}}d}}. \tag{17}$$

On the other hand, if the magnitude of the coil rotation frequency is much greater than the critical value then there are two different branches of solutions to the torque balance equation. The "high slip" branch satisfies

$$\omega \simeq \frac{|\omega_c|}{2}\left(1 + \sqrt{1 - \frac{|\Psi_v|^2}{|\Psi_{v2}|^2}}\right), \tag{18}$$

where

$$|\Psi_{v2}| = \frac{|\omega_c|\tau_{\mathrm{w}}}{4m}|\Psi_{v1}|. \tag{19}$$

The "low slip" branch satisfies

$$\frac{\omega\tau_{\mathrm{w}}}{2m} \simeq \frac{|\Psi_v|^2}{|\Psi_{v3}|^2} - \sqrt{\frac{|\Psi_v|^4}{|\Psi_{v3}|^4} - 1}, \tag{20}$$

where

$$|\Psi_{v3}| = \sqrt{\frac{|\omega_c|\tau_{\mathrm{w}}}{m}}\,|\Psi_{v1}|. \tag{21}$$

In the "high slip" branch of solutions the slip frequency is sufficient to exclude magnetic flux from the shaft to a large extent. As the field strength of the coils is gradually increased the slip frequency gradually reduces until at a critical field strength, corresponding to $|\Psi_v| = |\Psi_{v2}|$, the solution bifurcates to the "low slip" branch. In the "low slip" branch of solutions the slip frequency is low enough to permit magnetic flux to penetrate the shaft. As the field strength of the coils is gradually reduced the slip frequency gradually increases until at a critical field strength, corresponding to $|\Psi_v| = |\Psi_{v3}|$, the solution bifurcates to the "high slip" branch.

2.5 Phasing

The relationship between the two branches of solutions is sketched in Fig. 7. Note that the "high slip" to "low slip" bifurcation takes place at $\omega = |\omega_c|/2$; i.e. when the slip frequency is reduced to *one half* of its initial value (at zero coil field strength). The "low slip" to "high slip" bifurcation takes place at $\omega = 2m/\tau_{\mathrm{w}}$;
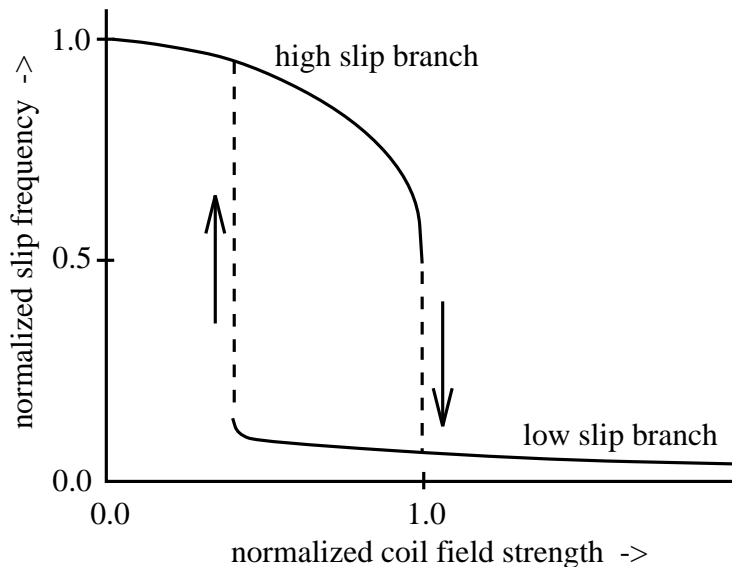
Figure 7: Schematic graph of the two branches of the torque balance equation plotted in normalized slip frequency, $\omega/|\omega_c|$, versus normalized coil field strength, $|\Psi_v|^2/|\Psi_{v2}|^2$, space

i.e. at the peak of the electromagnetic torque curve sketched in Fig. 6. Note also that there is a strong hysterises effect because the critical field strength for the upward (in slip frequency) bifurcation is much less than that for the downward bifurcation. Thus, if the coil field strength is just sufficient to cause a bifurcation to the "low slip" branch of solutions, and so allow magnetic flux to penetrate the shaft, then it must be reduced significantly before the flux is expelled from the shaft and a bifurcation back to the "high slip" branch takes place.

The origin of the bifurcations can easily be traced back to the non-monotonic variation of the electromagnetic torque with slip frequency which is sketched in Fig. 6. The "low slip" solutions lie on the low frequency side of the peak of the torque curve whereas the "high slip" solutions lie on the high frequency side. The two sets of solutions are separated by a "forbidden region" (which extends from the peak of the torque curve to a slip frequency of half the magnitude of the coil rotation frequency) in which there are no stable steady state solutions.

Conventional induction motors always operate in the regime where the coil "rotation" frequency is much greater than the critical value given by Eq. (15). In

other words, the coils always rotate fast enough to expel magnetic flux from the drive shaft when it is stationary. (Actually, the coils in an induction motor are stationary but are energized by phased oscillatory currents. This arrangement mimics the fields generated by a set of rotating coils.) An induction motor is designed to operate on the "low slip" branch of solutions where the drive shaft almost co-rotates with the coils. However, if too great a load is applied to the motor then it bifurcates to the "high slip" branch where there is very little effective coupling between the drive shaft and the coils. If the load is gradually reduced then a reverse transition eventually takes place. This switching between the two different branches of solutions is known as "phasing" in electrical engineering.

3 Driven Reconnection in Tokamaks

3.1 The Plasma Equilibrium

Consider a tokamak plasma equilibrium in which the "aspect ratio" (that is, the ratio of the major radius of the magnetic axis, R_0, to the minor radius of the plasma, a) is large. This implies that $\epsilon \equiv a/R_0 \ll 1$. Suppose that

$$\beta = \frac{\mu_0 p_0}{B_\phi{}^2} \sim O(\epsilon^2), \tag{22}$$

where p_0 is the plasma pressure on the magnetic axis, and B_ϕ is the approximately constant toroidal magnetic field strength. In the large aspect ratio, low-β, limit the equilibrium magnetic flux surfaces are of circular cross section (in the absence of external shaping coils) and are almost concentric. Thus, in this limit the equilibrium is well approximated as a cylindrical plasma which is periodic in the axial direction with periodicity length $2\pi R_0$. Conventional cylindrical polar coordinates are adopted in the following analysis. However, it is convenient to define a simulated toroidal angle $\phi = z/R_0$.

The equilibrium magnetic field is written $\mathbf{B} = (0, B_\theta(r), B_\phi)$. The associated equilibrium plasma current takes the form $\mathbf{j} = (0, 0, j_\phi(r))$, where

$$\mu_0 j_\phi(r) = \frac{1}{r} \frac{d(rB_\theta)}{dr}. \tag{23}$$

Equilibrium magnetic field lines satisfy the differential equation

$$\frac{d\phi}{d\theta} = q(r),\tag{24}$$

where the "safety factor"

$$q(r) = \frac{rB_\phi}{R_0 B_\theta}\tag{25}$$

parameterizes the helical pitch of the field lines. In a conventional tokamak plasma the safely factor is a monotonically increasing function of the flux surface radius r. Furthermore, $q \sim O(1)$.

3.2 Ideal MHD

Consider the response of a large aspect ratio, low-β, tokamak equilibrium to a helical error field with m periods in the poloidal direction and n periods in the toroidal direction. It is convenient to represent the perturbed magnetic field and the perturbed plasma current in terms of a flux function ψ (see Eqs. (1) and (2)). In the cylindrical limit it is reasonable to suppose that the plasma response possesses the same helicity as the error field. The error field is static in the laboratory frame (since it is generated by stationary field coils), so it is also reasonable to suppose that the plasma response is non time varying. Thus,

$$\psi(r,\theta,\phi,t) = \psi(r)\exp(\mathrm{i}\,(m\,\theta - n\,\phi)\,).\tag{26}$$

To a first approximation, the response of a conventional tokamak plasma to an external magnetic perturbation, such as an error field, is determined by the equations of ideal magnetohydodynamics (ideal MHD). These equations assume that the plasma acts like a perfectly conducting, inviscid, massless, fluid. In ideal MHD the linearized perturbed force balance equation takes the form

$$-\nabla\delta p + \delta\mathbf{j}\wedge\mathbf{B} + \mathbf{j}\wedge\delta\mathbf{B} = \mathbf{0},\tag{27}$$

where δp is the perturbed plasma pressure. The curl of the above relation yields the "cylindrical tearing mode equation",

$$\nabla^2\psi + \frac{\mu_0 j_\phi'}{B_\theta(nq/m - 1)}\,\psi = 0,\tag{28}$$

where $j'_\phi \equiv dj_\phi/dr$, and

$$\nabla^2 \psi \simeq \frac{1}{r}\frac{d}{dr}\left(r\,\frac{d\psi}{dr}\right) - \frac{m^2}{r^2}\,\psi \tag{29}$$

in the large aspect ratio limit.

In an induction motor an "error field" produced by a set of rotating field coils is able to exert a torque on a stationary conducting shaft by inducing eddy currents in the shaft. In a tokamak plasma the error field is stationary but, in general, the plasma is rotating. For instance, all tokamak plasmas are observed to possess a radial electric field, E_r, which when crossed with the equilibrium magnetic field gives rise to bulk plasma rotation. Furthermore, conventional plasma instabilities (such as tearing modes), which are locked into the frame of the plasma, are observed to propagate in the laboratory frame due to the plasma rotation. It appears likely, by analogy with an induction motor, that a stationary error field can exert a torque on a rotating tokamak plasma by inducing eddy currents in the plasma.

3.3   Electromagnetic Torques - I

Consider the flux surface averaged torque acting in the poloidal direction. This is given by

$$
\begin{aligned}
T_{\theta\,\mathrm{EM}}(r) &= \oint \oint r\,\hat{\boldsymbol{\theta}}\cdot(\mathbf{j}+\delta\mathbf{j}) \wedge (\mathbf{B}+\delta\mathbf{B})\, r d\theta\, R_0 d\phi \\
&= \oint \oint r\,\delta j_\phi \delta B_r\, r d\theta\, R_0 d\phi \\
&= -\frac{2\pi^2 m R_0}{\mu_0}\,\mathrm{Im}\left(r\,\nabla^2\psi\,\psi^*\right),
\end{aligned}
\tag{30}
$$

where use has been made of Eqs. (1), (2), and (26). Note that the torque is non-linear (i.e. it is proportional to the product of two perturbed quantities) and is, therefore, relatively small. According to the cylindrical tearing mode equation,

$$r\,\nabla^2\psi\,\psi^* = -\frac{\mu_0 r j'_\phi}{B_\theta(nq/m-1)}\,|\psi|^2. \tag{31}$$

Thus, $\mathrm{Im}\,(r\,\nabla^2\psi\,\psi^*) = 0$ and, therefore, $T_{\theta\,\mathrm{EM}} = 0$. Clearly, no torque can be exerted on flux surfaces located in a region of the plasma which is governed by the equations of ideal MHD. This is hardly a surprising result. A tokamak plasma differs from the drive shaft of an induction motor in one very important respect; namely, a tokamak plasma is non rigid. A force exerted inside a non rigid body is likely to cause a local displacement of the body. Such a displacement is opposed by inertia and viscosity. However, inertia and viscosity do not figure in the equations of ideal MHD (since they are regarded as being negligibly small). Thus, any force exerted inside an ideal plasma can be expected to cause the plasma to displace in such a manner that the force is set to zero. (Likewise, an electric field occurring inside a stationary perfect conductor causes currents to flow which rapidly redistribute charge in such a manner that the field is set to zero.)

3.4   The Breakdown of Ideal MHD

In ideal MHD the perturbed magnetic field is related to the plasma displacement, $\boldsymbol{\xi}$, via

$$\delta\mathbf{B} = \nabla \wedge (\boldsymbol{\xi} \wedge \mathbf{B}). \tag{32}$$

This equation is easily obtained by taking the curl of Ohm's law, linearizing, and then integrating with respect to time. The radial component of the above equation yields

$$\xi = \frac{\psi}{B_\theta(1 - nq/m)}, \tag{33}$$

where $\xi(r)\exp(\mathrm{i}\,(m\theta - n\phi))$ is the radial plasma displacement. To lowest order the plasma is incompressible (since the strong toroidal magnetic field resists compression), so $\nabla\!\cdot\!\boldsymbol{\xi} = \mathbf{0}$, which enables the poloidal plasma displacement to be calculated from the radial displacement (the toroidal displacement is negligible in the large aspect ratio limit). Equation (33) specifies how a tokamak plasma can displace in response to an external magnetic perturbation in such a manner that no eddy currents are induced and, therefore, no torque is exerted inside the plasma.

According to Eq. (33) the plasma displacement required to prevent eddy currents becomes infinite on any flux surface characterized by $q(r_s) = m/n$. Such a surface is called a "rational" flux surface, since on it the magnetic winding number q takes the rational value m/n. On a rational surface the helical pitch of the equilibrium magnetic field exactly matches that of the phase of the externally applied magnetic perturbation. It is clear from Eq. (28) that the cylindrical tearing mode equation becomes singular when $q = m/n$, indicating that ideal MHD is invalid in the immediate vicinity of a rational surface. It is, therefore, possible for an error field to exert a torque on the plasma in such a region.

Ideal MHD breaks down in the immediate vicinity of a rational flux surface because the extremely large displacement of the plasma required by Eq. (33) to suppress eddy currents is prevented by plasma inertia and viscosity. Suppose that plasma inertia and viscosity invalidate Eq. (33) in a thin layer of thickness δ_s centred on the rational surface, radius r_s Thus, the plasma displacement inside the layer is insufficient to prevent eddy currents from flowing. Clearly, the plasma in the layer acts very much as if it were rigid. By analogy with Eq. (4), it is helpful to define a "time constant" of the layer,

$$\tau_s = \mu_0 \sigma(r_s) r_s \delta_s, \tag{34}$$

where $\sigma(r)$ is the plasma electrical conductivity. There is an equivalent limit to the "thin shell" limit, described in Eq. (5), in which there is negligible radial variation of the magnetic flux function $\psi(r)$ across the layer. This limit is usually called the "constant-ψ" limit, and is valid provided that (cf. Eq. (5))

$$\frac{\delta_s}{r_s} \ll |\omega|\tau_s \ll \frac{r_s}{\delta_s}. \tag{35}$$

The slip frequency ω (which is defined in an analogous manner to the slip frequency in Section 2) is minus the oscillation frequency of the helical error field in the rotating frame of the plasma at the rational surface. Thus,

$$\omega = m\,\Omega_\theta(r_s) - n\,\Omega_\phi(r_s), \tag{36}$$

where $\Omega_\theta(r)$ and $\Omega_\phi(r)$ are the poloidal and toroidal angular rotation frequencies

of the plasma, respectively. By analogy with Eq. (6),

$$\left[r \frac{d\psi}{dr} \right]_{r_s - \delta_s/2}^{r_s + \delta_s/2} = \mathrm{i}\,\omega \tau_s\,\Psi_s, \tag{37}$$

where $\Psi_s \equiv \psi(r_s)$.

3.5 Magnetic Reconnection

The quantity Ψ_s has a special significance which can easily be appreciated by mapping out the magnetic field lines in the immediate vicinity of the rational surface. Figure 8 shows the field lines plotted as functions of the helical angle $\xi = m\theta - n\phi$ and $X = (r - r_s)/W_s$, where

$$W_s = 4\sqrt{\frac{m\,R_0\,|\Psi_s|}{n B_\phi s}}, \tag{38}$$

and $s = (d\ln q/d\ln r)_{r_s}$. It can be seen that magnetic reconnection has taken place in Fig. 8, giving rise to a chain of magnetic islands whose full width W_s is proportional to the square root of $|\Psi_s|$. In fact, Ψ_s is the reconnected magnetic flux at the rational surface. The magnetic island chain is stationary in the laboratory frame since it is "locked" to the non rotating error field.

Magnetic reconnection, and the consequent formation of magnetic islands, has a deleterious effect on the confinement properties of a tokamak plasma equilibrium. This is because particles are able to travel radially from one side of an island to the other by flowing along field lines, which is a relatively fast process, instead of diffusing across flux surfaces, which is a relatively slow process.

3.6 Linear Layer Theory

Linear layer analysis, employing single fluid equations which take into account the effects of plasma inertia, viscosity, and resistivity, shows that Eqs. (34)–(37)
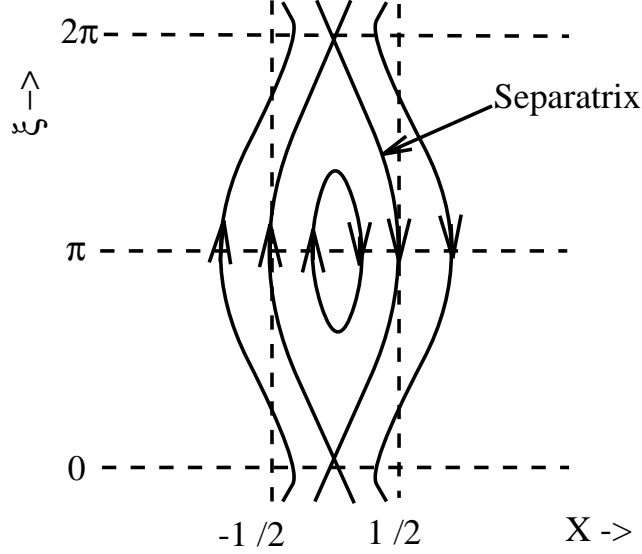
Figure 8: Reconnected magnetic field lines in the vicinity of the rational flux surface, plotted as a function of $\xi = m\theta - n\phi$ and $X = (r - r_s)/W_s$

are essentially correct, and that the layer width is given by

$$\frac{\delta_s}{r_s} = 2.104 \left(\frac{\tau_H^2}{\tau_R \tau_V} \right)^{1/6} , \tag{39}$$

where $\tau_H = (R_0/B_\phi)\sqrt{\mu_0 \rho(r_s)}/ns$ is the hydromagnetic timescale, $\tau_R = \mu_0 r_s^2 \sigma(r_s)$ the resistive diffusion timescale, and $\tau_V = r_s^2 \rho(r_s)/\mu(r_s)$ the viscous diffusion timescale. Here, $\rho(r)$ is the plasma mass density, and $\mu(r)$ the cross flux surface viscosity. Equation (39) is only valid when $\tau_V \ll \tau_R$. In a conventional tokamak plasma the hydromagnetic timescale is about 10^{-7} seconds; the resistive timescale is anything from five to eight orders of magnitude greater than the hydromagnetic timescale (the resistive timescale is longer in larger, hotter devices); the viscous timescale is usually an order of magnitude less than the resistive timescale. It follows that the layer width given in Eq. (39) is a small fraction of the plasma minor radius. Linear layer theory is only valid if the island width W_s is much less than the linear layer width δ_s. Thus, linear theory only holds prior to any substantial magnetic reconnection.

3.7 Asymptotic Matching

In the ideal region (i.e. everywhere apart from the singular layer and the external coils which maintain the error field) the flux function $\psi(r)$ satisfies the cylindrical tearing mode equation, (28). It is convenient to assume that there is negligible plasma current outside the rational surface (i.e. $j_\phi = 0$ for $r > r_s$). This approximation is only valid if the rational surface lies in the outer regions of the plasma (i.e. $r_s/a \gtrsim 0.6$). Thus, for $r > r_s$ the flux function is "vacuum like" and is therefore made up of a linear combination of r^{+m} and r^{-m} type solutions.

The most general ideal solution is written

$$\psi(r) = \Psi_s \psi_{\text{plasma}}(r) + \psi_{\text{shield}}(r). \tag{40}$$

The plasma solution $\psi_{\text{plasma}}(r)$ satisfies physical boundary conditions at $r = 0$ and $r \to \infty$ (in the absence of any error field) and is normalized to unity at the rational surface (i.e. $\psi_{\text{plasma}}(r_s) = 1$). In general, the plasma solution has a gradient discontinuity at the rational surface. It is helpful to define

$$\Delta' = \left[r \, \frac{d\psi_{\text{plasma}}}{dr} \right]_{r_{s-}}^{r_{s+}}. \tag{41}$$

This quantity is know as the "tearing stability index". According to conventional tearing mode theory, if $\Delta' > 0$ then the plasma spontaneously reconnects at the rational surface to form a magnetic island. Note that such an island is locked into the frame of the plasma at the rational surface and, therefore, rotates in the laboratory frame. The oscillation frequency of the magnetic field associated with a spontaneously created magnetic island is

$$\omega_0 = m \, \Omega_{\theta\,0}(r_s) - n \, \Omega_{\phi\,0}(r_s), \tag{42}$$

where $\Omega_{\theta\,0}$ and $\Omega_{\phi\,0}$ are the poloidal and toroidal angular rotation velocities of the plasma in the absence of an error field. In the following, it is assumed that $\Delta' < 0$, so that the plasma is intrinsially tearing stable. In this situation any magnetic reconnection which takes place inside the plasma is due solely to the externally applied error field. Such reconnection is known as "driven reconnection".
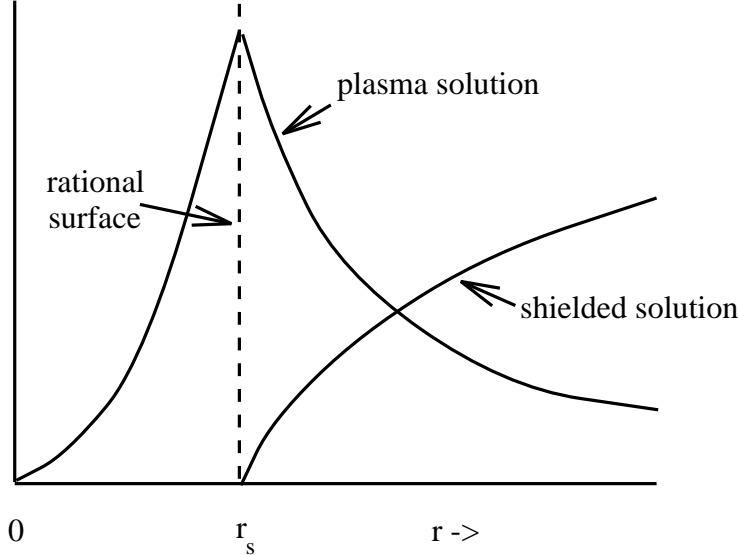
Figure 9: A schematic diagram showing typical plasma and shielded solutions

The shielded solution $\psi_{\text{shield}}(r)$ satisfies physical boundary conditions in the presence of the error field, with zero reconnection inside the plasma (i.e. $\psi_{\text{shield}}(r_s) = 0$). The error field is such that in the absence of plasma the flux at radius r_s is Ψ_v. This quantity is termed the "vacuum flux" and affords a convenient means to parameterize the strength of the error field. It is easily demonstrated that $\psi_{\text{shield}} = 0$ inside the rational surface, and that

$$\psi_{\text{shield}}(r) = \Psi_v \left[\left(\frac{r}{r_s} \right)^{+m} - \left(\frac{r}{r_s} \right)^{-m} \right] \tag{43}$$

for $r_c > r > r_s$, where $r_c > a$ is the radius of the coils which maintain the error field. The plasma and shielded solutions are sketched in Fig. 9.

Ideal MHD in the region outside the layer gives

$$\left[r \, \frac{d\psi}{dr} \right]_{r_{s-}}^{r_{s+}} = \Delta' \, \Psi_s + 2m \, \Psi_v, \tag{44}$$

where use has been made of Eqs. (40), (41), and (43). Resistive MHD inside the

21

layer yields Eq. (37). These two relations can be combined to give

$$\Psi_s = \frac{2m}{-\Delta' + i\,\omega\tau_s}\,\Psi_v. \tag{45}$$

Note the similarity between this formula and Eq. (9).

According to Eq. (45), if the slip frequency ω (i.e. minus the oscillation frequency of the error field in the rotating frame of the plasma; see Eq.(36)) is zero then the reconnected flux Ψ_s attains its maximum value

$$\Psi_s = \Psi_{\text{full}} = \left(\frac{2m}{-\Delta'}\right)\Psi_v. \tag{46}$$

This is usually termed the "fully reconnected flux". In general, $-\Delta' < 2m$ in tearing stable plasmas. It follows that $|\Psi_s| > |\Psi_v|$. In other words, the plasma *amplifies* the error field so that the flux at the rational surface exceeds that obtained at the same radius in the absence of plasma.

Equation (45) also implies that if the slip frequency greatly exceeds the critical value $(-\Delta')/\tau_s$ then the eddy currents which are induced in the resistive layer centred on the rational surface effectively suppress magnetic reconnection, so that $|\Psi_s|$ becomes much less than its fully reconnected value $|\Psi_{\text{full}}|$. This is a very significant result since it implies that the application of a helical error field to a rotating tokamak plasma does *not* necessarily give rise to significant magnetic reconnection inside the plasma. Instead, it is possible for strong eddy currents to be excited in the vicinity of the rational surface which prevent any reconnection.

3.8   Electromagnetic Torques - II

According to Eqs. (30), (37), and (45) the net poloidal electromagnetic torque acting in the vicinity of the rational surface is given by

$$\delta T_{\theta\,\text{EM}} = \int_{r_{s-}}^{r_{s+}} T_\theta\,dr = -\frac{8\pi^2 m^3 R_0}{\mu_0}\frac{\omega\tau_s}{(-\Delta')^2 + (\omega\tau_s)^2}\,|\Psi_v|^2. \tag{47}$$

Note the similarity between the above equation and Eq. (11). The torque exhibits the same non monotonic variation with slip frequency as that shown in Fig. 6 for

22

the case of an induction motor. If the slip frequency is zero then the torque is zero because there is no differential rotation between the plasma and the error field and so no eddy currents are excited. The torque initially increases with increasing slip frequency because of the increasing strength of induced eddy currents. However, above a critical value of the slip frequency the torque starts to decrease with increasing slip frequency because the eddy currents become strong enough to suppress magnetic reconnection (so there is no magnetic field to cross with the eddy currents and produce a torque). This critical value of the slip frequency is $(-\Delta')/\tau_s$; i.e. about the same as the growth rate of a naturally unstable tearing mode.

Consider a torus made up of a completely rigid material such as metal. It is clear that the torus is free to rotate toroidally. However, poloidal rotation is impossible because such rotation requires compression of the material as it moves from the outboard to the inboard side of the torus. A tokamak plasma is not a rigid body, but it does possess strong parallel (to the magnetic field) viscosity which opposes the plasma compression associated with poloidal rotation. In fact, in conventional tokamak plasmas this viscosity is sufficiently large to prevent any poloidal rotation. Thus, in practice, the plasma does not respond to the poloidal component of the electromagnetic torque exerted on it by the error field. However, the plasma is free to respond to the toroidal component of the electromagnetic torque (by changing its toroidal rotation). In the constant-ψ approximation the net poloidal and toroidal electromagnetic torques acting on the resistive layer centred on the rational surface are given by

$$\delta T_{\theta\,\text{EM}} \quad = \quad \oint \oint r \, \overline{\delta j_\phi} \, \delta B_r \, rd\theta \, R_0 d\phi, \tag{48a}$$

$$\delta T_{\phi\,\text{EM}} \quad = \quad - \oint \oint R_0 \, \overline{\delta j_\theta} \, \delta B_r \, rd\theta \, R_0 d\phi, \tag{48b}$$

where

$$\overline{\delta j_{\theta,\,\phi}} = \int_{r_{s-}}^{r_{s+}} \delta j_{\theta,\,\phi} \, dr. \tag{49}$$

Radial integration of $\nabla \cdot \delta \mathbf{j} = \mathbf{0}$ across the layer yields

$$\frac{m}{r} \, \overline{\delta j_\theta} - \frac{n}{R_0} \, \overline{\delta j_\phi} = 0. \tag{50}$$

Thus,

$$\delta T_{\phi\,\mathrm{EM}} = -\frac{n}{m}\,\delta T_{\theta\,\mathrm{EM}} = \frac{8\pi^2 n m^2 R_0}{\mu_0}\frac{\omega\tau_s}{(-\Delta')^2 + (\omega\tau_s)^2}\,|\Psi_v|^2, \qquad (51)$$

where use has been made of Eq. (47).

3.9 Viscous Torques

Suppose that the change in the toroidal angular rotation profile of the plasma induced by the error field is $\Delta\Omega_\phi(r)$. It is assumed that perpendicular viscosity acts to relax the rotation profile back to that of the unperturbed plasma (i.e. it tries to make $\Delta\Omega_\phi$ zero). It follows that

$$\frac{d}{dr}\left(r\mu\,\frac{d\Delta\Omega_\phi}{dr}\right) = 0 \qquad (52)$$

in a steady state, except in the immediate vicinity of the rational surface where the electromagnetic torque acts. Here, $\mu(r)$ is the perpendicular (to the magnetic field) viscosity of the plasma. The boundary condition at the edge of the plasma $r = a$ is

$$\Delta\Omega_\phi(a) = 0. \qquad (53)$$

In other words, the plasma rotation is clamped at the edge and is not substantially modified by the error field. It is easy to demonstrate theoretically that this is a reasonable assumption. There is also good experimental evidence that the edge plasma rotation is unaffected by error fields.

The localized toroidal electromagnetic torque acting in the vicinity of the rational surface gives rise to a localized viscous torque:

$$\delta T_{\phi\,\mathrm{VS}} = 4\pi^2 R_0 \left[r\mu R_0{}^2\,\frac{d\Delta\Omega_\phi}{dr} \right]_{r_{s-}}^{r_{s+}}. \qquad (54)$$

Note that this formula implies an effective discontinuity in the radial gradient of the toroidal rotation profile across the rational surface.

The most general solution of Eq. (52), subject to the boundary condition (53), is

$$\Delta\Omega_\phi(r) = \Delta\Omega_{\phi s} \tag{55}$$

for $r < r_s$, and

$$\Delta\Omega_\phi(r) = \Delta\Omega_{\phi s} \int_r^a \frac{dr}{r\mu} \bigg/ \int_{r_s}^a \frac{dr}{r\mu} \tag{56}$$

for $r_s < r < a$. Note that the modification to the toroidal rotation profile of the plasma induced by an error field is constant inside the rational surface and highly sheared outside the rational surface. Equations (54)–(56) yield the following expression for the viscous torque:

$$\delta T_{\phi\,\mathrm{VS}} = -4\pi^2 R_0{}^3 \,\Delta\Omega_{\phi s} \bigg/ \int_{r_s}^a \frac{dr}{r\mu}\ . \tag{57}$$

The above expression is calculated on the assumption that the velocity profile has sufficient time to *relax* across the whole plasma cross section under the influence of viscosity. This assumption is reasonable because the viscous relaxation timescale in tokamak plasmas is generally an order of magnitude less than the magnetic reconnection timescale. Thus, the velocity profile always has time to relax during the formation of an error field driven magnetic island.

The error field induced change in the toroidal rotation of the plasma gives rise to a modification of the slip frequency (i.e. minus the oscillation frequency of the error field seen in the rotating frame of the plasma at the rational surface). According to Eqs. (36) and (42) (assuming that poloidal flow is strongly damped)

$$\omega = \omega_0 - n\Delta\Omega_{\phi s}, \tag{58}$$

where ω_0 is the oscillation frequency of a naturally unstable (i.e. $\Delta' > 0$) m/n tearing mode in the unperturbed plasma. This frequency is termed the "natural frequency".

3.10 Torque Balance

In a steady state the electromagnetic and viscous torques acting on the plasma in the vicinity of the rational surface must balance. Thus,

$$\delta T_{\phi\,\text{EM}} + \delta T_{\phi\,\text{VS}} = 0. \tag{59}$$

Equations (51), (57), and (58) yield

$$\frac{2n^2 m^2 \tau_s \left(\int_{r_s}^a dr/r\mu\right) |\Psi_v|^2}{\mu_0 R_0^{\,2}(-\Delta')^2} \frac{\omega}{1 + (\omega\tau_s/(-\Delta'))^2} = \omega_0 - \omega. \tag{60}$$

This equation is analogous to Eq. (14) which governs the behaviour of an induction motor.

It is easily demonstrated that there is a critical natural frequency for the m/n tearing mode; namely,

$$(\omega_0)_{\text{crit}} = \frac{3\sqrt{3}\,(-\Delta')}{\tau_s}. \tag{61}$$

If the natural frequency is much less than this critical value then the slip frequency never gets sufficiently large to suppress magnetic reconnection inside the plasma. Consequently, $\Psi_s \simeq \Psi_{\text{full}}$. In other words, full reconnection is always achieved. On the other hand, if the natural frequency is much greater than the critical value then there are two quite different branches of solutions to the torque balance equation. The "unreconnected" branch satisfies

$$\omega \simeq \frac{\omega_0}{2}\left(1 + \sqrt{1 - \frac{|\Psi_v|^2}{|\Psi_{v1}|^2}}\right), \tag{62}$$

where

$$|\Psi_{v1}| = \frac{\omega_0 R_0}{2nm}\sqrt{\frac{\mu_0 \tau_s}{2\left(\int_{r_s}^a dr/r\mu\right)}}. \tag{63}$$

On this branch $|\Psi_s| \ll |\Psi_{\text{full}}|$, so very little magnetic reconnection takes place within the plasma. The "fully reconnected" branch satisfies

$$\frac{\omega\tau_s}{(-\Delta')} \simeq \frac{|\Psi_v|^2}{|\Psi_{v2}|^2} - \sqrt{\frac{|\Psi_v|^4}{|\Psi_{v2}|^4} - 1}, \tag{64}$$

where

$$|\Psi_{v2}| = \sqrt{\frac{8\,(-\Delta')}{\omega_0 \tau_s}}\,|\Psi_{v1}| = \frac{R_0}{nm}\sqrt{\frac{\mu_0 \omega_0 (-\Delta')}{(\int_{r_s}^{a} dr/r\mu)}}. \tag{65}$$

On this branch $|\Psi_{\text{full}}| > |\Psi_s| > |\Psi_{\text{full}}|/\sqrt{2}$, so almost full reconnection is achieved within the plasma.

3.11   Formation of Locked Islands

The relationship between the two branches of solutions is similar to that sketched in Fig. 7 for an induction motor (the "high slip" branch is equivalent to the "unre-connected" branch, the "low slip" branch is equivalent to the "fully reconnected" branch, and the coil field strength is equivalent to the error field strength).

Suppose that a low amplitude error field is applied to a tokamak plasma and the error field strength is then gradually ramped up. According to the previous analysis, there is initially almost no driven reconnection inside the plasma. In other words, the error field does not give rise to the formation of a magnetic island. Instead, strong eddy currents are excited in the vicinity of the rational surface which effectively shield the error field from the interior of the plasma (i.e. the region $r \leq r_s$). This effect is a direct consequence of the *rotation* of the plasma with respect to the stationary error field.

The eddy currents induced in the plasma by the error field give rise to a localized electromagnetic torque which acts to slow down the plasma rotation. According to Eqs. (36) and (62),

$$\Omega_\phi(r_s) = \Omega_{\phi\,0}(r_s)\left(\frac{1}{2} + \frac{1}{2}\sqrt{1 - \frac{|\Psi_v|^2}{|\Psi_{v1}|^2}}\right), \tag{66}$$

where $\Omega_\phi(r_s)$ is the plasma toroidal angular rotation velocity at the rational surface, and $\Omega_{\phi\,0}(r_s)$ is the corresponding velocity in the absence of an error field. Note that $|\Psi_v|$ is related to, b_r, the m/n harmonic of the radial error field at the rational surface in the absence of plasma, via $b_r = m|\Psi_v|/r_s$. It is assumed that any poloidal rotation of the plasma is rapidly damped by parallel plasma

viscosity. According to Eq. (66), the plasma rotation at the rational surface gradually slows down as the error field amplitude is ramped up until the rotation is reduced to one half of its original value, at which point there is a bifurcation to the fully reconnected branch of solutions. The critical value of b_r required to trigger such a bifurcation is

$$b_{r\,\text{lock}} = \frac{\omega_0 R_0}{2 n r_s} \sqrt{\frac{\mu_0 \tau_s}{2\left(\int_{r_s}^a dr/r\mu\right)}}. \tag{67}$$

In the fully reconnected branch of solutions the error field induced electromagnetic torque is sufficiently large to effectively arrest the rotation of the plasma at the rational surface, so that $\Omega_\phi(r_s) \ll \Omega_{\phi 0}(r_s)$. The weak differential rotation between the plasma and the error field leads to eddy currents which are too feeble to suppress magnetic reconnection. In this situation, a stationary magnetic island forms inside the plasma. If the error field strength greatly exceeds the critical value given in Eq. (67) then the driven island width attains its fully reconnected value,

$$W_{\text{full}} = 4\sqrt{\frac{2 m r_s R_0\, b_r}{n B_\phi s\left(-\Delta'\right)}}. \tag{68}$$

Note that, in this case, the driven island has the same phase as the "vacuum island" obtained by adding the vacuum error field to the equilibrium magnetic field and then tracing field lines. Once a stationary, or "locked", magnetic island has formed inside the plasma the error field strength must be reduced significantly below the critical value given in Eq. (67) before the island heals and the strong eddy currents which prevent further magnetic reconnection reform in the vicinity of the rational surface. The critical value of b_r below which a bifurcation to the unreconnected branch of solutions is triggered is

$$b_{r\,\text{unlock}} = \frac{R_0}{n r_s} \sqrt{\frac{\mu_0 \omega_0\left(-\Delta'\right)}{\left(\int_{r_s}^a dr/r\mu\right)}}. \tag{69}$$

Just prior to the bifurcation the locked island is phase shifted with respect to the vacuum island by $45°$ and its width is $W_{\text{full}}/2^{1/4}$.

3.12 Non Linear Effects

The results described in the previous subsection are dependent on linear layer theory, which is only valid if the width of the stationary error field driven magnetic island (see Eq. (38)) is much less than the width of a linear layer (see Eq. (39)). This is a reasonable assumption for the unreconnected branch of solutions, on which the strong eddy currents induced in the vicinity of the rational surface suppress magnetic reconnection and prevent the formation of a magnetic island. However, linear layer theory is likely to break down for the fully reconnected branch of solutions, on which the eddy currents are too weak to prevent the formation of an error field driven magnetic island. This suggest that Eq. (67), which gives the critical radial error field to induce a stationary magnetic island in a rotating tokamak plasma, is valid but Eq. (69), which gives the critical radial error field for the expulsion of a stationary magnetic island from a rotating plasma, may be inaccurate. In fact, non linear analysis shows that the correct form for the critical error field below which a stationary magnetic island is expelled from a rotating plasma is

$$b_{r\,\text{unlock}} = \left(\frac{2m}{-\Delta'} \right)^{1/4} \frac{R_0}{n r_s} \sqrt{\frac{\mu_0 \omega_0 \, (-\Delta')}{(\int_{r_s}^{a} dr/r\mu)}}, \tag{70}$$

which only differs slightly from the expression given in Eq. (69). In non linear theory, as in linear theory, just prior to expulsion the stationary island is phase shifted with respect to the vacuum island by $45°$ and its width is $W_{\text{full}}/2^{1/4}$.

Suppose that on the unreconnected branch of solutions the suppression of magnetic reconnection is not sufficient to make the non linear island width less than the linear layer width. This situation may arise in large hot tokamak plasmas, where the linear layers become extremely narrow. A stationary magnetic island can only form if the electromagnetic torque exerted in the vicinity of the rational surface is sufficiently large to arrest the local plasma rotation, because plasma cannot flow across the island separatrix. If the torque is too small then the island is "suppressed" and a highly non linear structure, whose width is similar to the linear layer width, forms in the vicinity of the rational surface. Careful numerical simulations of the suppressed island state by R.D. Parker indicate that its behaviour is not too dissimilar to that of a linear layer. For instance, Parker

finds numerically that $b_{r\,\text{lock}} \propto \omega_0\,\tau_R^{0.4}\tau_H^{1.27}/\tau_V^{0.67}$ whereas the scaling predicted by linear layer theory is $b_{r\,\text{lock}} \propto \omega_0\,\tau_R^{0.42}\tau_H^{1.16}/\tau_V^{0.58}$ (see Eqs. (34), (39), and (67)).

3.13   Conclusions

The basic question posed in the introduction was "What effect does an error field have on the nested equilibrium magnetic flux surfaces of a tokamak plasma?". This question can now be answered.

The fact that tokamak plasmas rotate in the laboratory frame affords them some measure of protection against error field driven magnetic reconnection. Low amplitude error fields are shielded from the interior of the plasma by eddy currents localized in the vicinity of the rational surfaces. These eddy currents prevent the formation of magnetic islands and any associated degradation of the confinement properties of the plasma equilibrium. The eddy currents also give rise to a torque acting on the plasma which slows down the rotation. As the error field amplitude is gradually ramped up the plasma gradually slows down, with little or no driven reconnection, until a critical error field amplitude is reached. At the critical amplitude the plasma rotation is suddenly arrested and driven magnetic reconnection is enabled, giving rise to the formation of stationary magnetic islands with an associated degradation of the plasma confinement. The error field strength must be reduced significantly below the critical value before the stationary islands are expelled from the plasma and the undegraded plasma confinement is again achieved.

Tokamak plasmas rotate for many diffenent reasons. Many tokamaks are heated by unbalanced neutral beam injection (NBI), in which high energy (e.g. 75 k eV) neutral particles are injected into the plasma preferentially in one toroidal direction. Although this is primarily a heating scheme it can give rise to bulk toroidal plasma rotation with velocities in excess of 10 km/s. Such large velocities invariably lead to the break down of the constant-ψ approximation, which requires the inequality (35) to be satisfied, so a more sophisticated analysis than that given above is generally required. In this situation the torque exerted on the plasma by the error field can be thought of as due to the absorption of slow Alfvèn waves

traveling preferentially in one direction (this is how the error field appears to the rotating plasma).

In ohmically heated tokamaks the plasma *appears* to rotate at the electron diamagnetic velocity,[2]

$$\mathbf{v}_* = \frac{\nabla p_e \wedge \mathbf{B}}{n_e e B^2},\tag{71}$$

because of two fluid effects (i.e. the fact that the plasma is actually made up of free electrons and ions). Here, p_e is the electron pressure, and n_e is the number density of electrons. Since the diamagnetic rotation is apparant, rather than real, it is not subject to poloidal flow damping. The diamagnetic velocity is much less than a typical neutral beam induced velocity but it is nevertheless sufficient to prevent driven reconnection by low amplitude error fields (i.e. ω_0 is much greater than the critical value given in Eq. (61)). Fortunately, this velocity is generally not large enough to invalidate the constant-ψ approximation. The natural frequency of tearing modes in an ohmically heated plasma is of order

$$\omega_0 \sim \frac{m}{r_s} v_{*\,\theta} \sim \frac{m T_e(r_s)(\eta_{n_e} + \eta_{T_e})}{e B_\phi r_s^{\,2}},\tag{72}$$

where T_e is the electron temperature, $\eta_{n_e} = (d \ln n_e / d \ln r)_{r_s}$, and $\eta_{T_e} = (d \ln T_e / d \ln r)_{r_s}$. Note that $\omega_0 \propto T_e/B_\phi a^2$ for similar plasma discharges on different devices. This suggests that the natural frequencies of tearing modes in an ohmically heated tokamak are strongly decreasing functions of the dimensions of the device (the variation of T_e/B_ϕ with machine size is relatively weak). According to Eq. (67), large ohmically heated plasmas are likely to be far more susceptible to error field driven reconnection, and the associated degradation of plasma confinement, than small plasmas. Clearly, accurate positioning of field coils and proper design of coil feeds is far more important in large tokamaks than in small tokamaks.

In very large (i.e. $a > 1$ m) ohmically heated tokamaks the critical error field strength needed to induce a locked island, given by Eq. (67), falls below a gauss, which is about the lowest level to which an error field can practically be reduced by accurate positioning of field coils. Thus, in very large tokamaks active measures may be required to cancel out the error field. Note that only those m/n harmonics

---

[2]This is a gross oversimplification of a rather complicated phenomenon.

of the error field which possess rational surfaces lying within the plasma need to be eliminated. It is relatively straightforward to design a set of correction coils to achieve this.

4   Experimental Results

Figure 10 shows data obtained from the COMPASS-C tokamak (a small tokamak). In this discharge an artificial $m = 2/n = 1$ error field is applied to the plasma with the aid of external saddle coils (the intrinsic error field is negligibly small). The first trace shows the current flowing in the saddle coils. The current is first ramped up to an flattop level for which the associated error field strength lies below the locking threshold. The current is then increased such that the locking threshold is exceeded at about time (a). The second trace shows the central soft x-ray emission. Prior to time (a) the emission is high, indicating good plasma energy confinement. However, the emission collapses after time (a), implying a severe degradation in confinement. The fifth trace shows the $n = 1$ component of the radial magnetic field at the edge of the plasma measured relative to that obtained when the saddle coils are pulsed in the absence of plasma. Prior to time (a) the signal is negative. This indicates that reconnection has not taken place inside the plasma. Instead, strong eddy currents flowing in the vicinity of the rational surface shield the error field from the plasma interior (and also reduce the radial field at the edge of the plasma relative to that obtained in the absence of plasma). After time (a) the signal becomes positive. This indicates the decay of the eddy currents and the formation of a locked magnetic island (this tends to increase the radial field at the plasma edge relative to that obtained in vacuum). The final trace shows the ion impurity toroidal rotation velocity. This is related to the "plasma" rotation velocity (which, in this case, really means the rotation velocity of the electron fluid) by a simple offset. There is a slight reduction in the rotation prior to time (a) (which is difficult to see in the figure) and a much more dramatic reduction at time (a). The error field is suddenly switched off at time (b). The data indicates that the stationary magnetic island gradually decays away. The island is also forced to rotate as the plasma rotation is gradually re-established. Note that the confinement impoves as soon as the island has
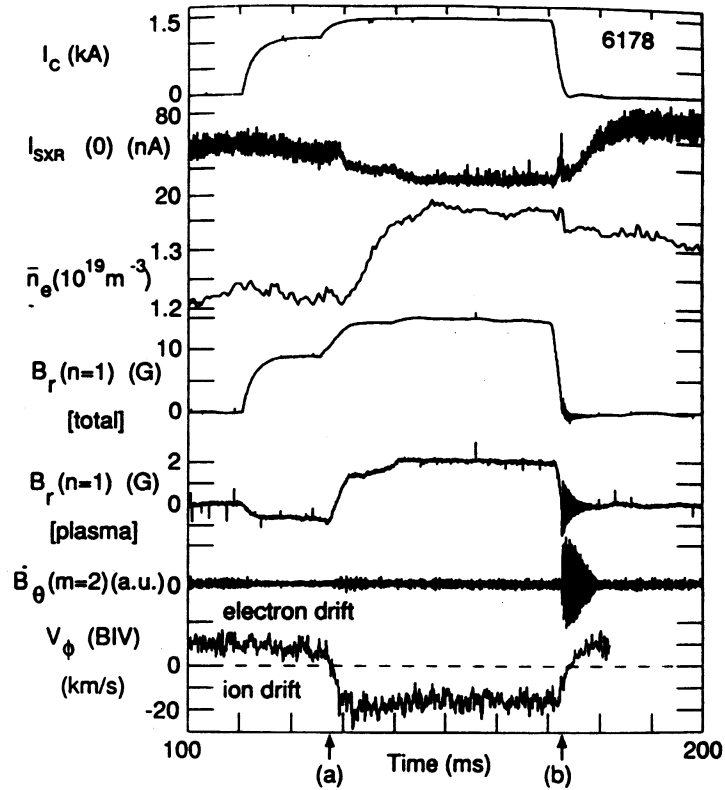
Figure 10: Data obtained from the Compass-C tokamak. Figure 2 reproduced from Nucl. Fusion **32**, 2091 (1992).

disappeared. Although it is difficult to see in the figure, the critical error field strength at which the island "unlocks" (i.e. starts to rotate and simultaneously decay away) is far smaller than that required at time (a) to produce a locked island from scratch.

It can be seen that all of the major predictions of Section 3 are borne out experimentally. The critical error field amplitude required to induce a locked island lies within a factor two of that predicted by formula (67). Error field experiments have also been performed on the DIII-D tokamak (a medium sized tokamak) and the JET tokamak (a large tokamak). The data obtained from these experiments is also in accordance with the theory outlined in Section 3.

5 Summary

A rotating tokamak plasma can exist in one of two possible states in the presence of an error field. In the "unreconnected" state the plasma rotates, strong eddy currents shield the plasma interior from the error field, and there is little induced magnetic reconnection. In the "fully reconnected" state the plasma rotation is arrested, the eddy currents are weak, and a stationary magnetic island is introduced into the plasma. The plasma can "jump" between these two states at certain critical values of the error field strength. This behaviour is analagous to the well known phenomenon of "phasing" in induction motors. The origin of the "jumps" lies in the highly non monotonic variation of the electromagnetic braking torque acting on the plasma with the plasma rotation velocity.

The effects of error fields on tokamak plasmas have been investigated extensively on three different devices; COMPASS-C (a small tokamak), DIII-D (a medium sized tokamak), and JET (a large tokamak). By and large, the predictions of Section 3 are borne out experimentally. In all three tokamaks there is a critical error field strength above which the plasma rotation suddenly collapses across the whole cross section and a stationary magnetic island is introduced into the plasma giving rise to a degradation of confinement. The observed critical error field strength for the creation of a locked island lies within a factor two of the theoretical prediction (67). The critical field strength is observed to increase with increasing plasma density, which is explicable if high density plasmas are more viscous than low density plasmas (see Eq. (67)). The critical field strength is also observed to decrease markedly with increasing machine size, as expected. This suggests that error fields may pose a particular problem for next generation tokamaks which are likely to be significantly larger than present day devices.

Acknowledgment

Bibliography

Overview of Tokamaks: J.A. Wesson, *Tokamaks*, (Clarendon Press, Oxford, 1987).

Bifurcations in Induction Devices: C.G. Gimblett, and R.S. Peckover, Proc. R. Soc. London, Ser. A Math. Phys. Sci. **368**, 75 (1979).

Overview of MHD Stability Theory: J.A. Wesson, Nucl. Fusion **18**, 87 (1978).

Basic Tearing Mode Theory: H.P. Furth, J. Killeen, and M.N. Rosenbluth, Phys. Fluids **6**, 459 (1963).

Overview of Linear Layer Theory: R. Fitzpatrick, Phys. Plasmas **1**, 3308 (1994) (Appendix B).

Basic Non Linear Tearing Mode Theory: P.H. Rutherford, Phys. Fluids **16**, 1903 (1973).

Degradation of Confinement by Magnetic Islands: Z. Chang, and J.D. Callen, Nucl. Fusion **30**, 219 (1990).

Theory of Error Field Driven Reconnection: R. Fitzpatrick, in *Theory of Fusion Plasmas*, Proc. Joint Varenna-Lausanne Int. Workshop, Varenna 1992, (Editrice Compositiori, Bolagna, 1992), 147;
T.H. Jensen, A.W. Leonard, and A.W. Hyatt, Phys. Fluids B **5**, 1239 (1993).

Simulation of Error Field Driven Reconnection: R.D. Parker, in *1992 International Conference on Plasma Physics*, Proc. Conf. Innsbruck 1992, (European Physical Society, Geneva, 1992), Part I, 427.

Two Fluid Effects in Tearing Mode Theory: G. Ara, B. Basu, B. Coppi, G. Laval, M.N. Rosenbluth, and B.V. Waddell, Ann. Phys. (NY) **112**, 443 (1978).

Compass-C Results: T.C. Hender, R. Fitzpatrick, A.W. Morris, *et al.*, Nucl. Fusion **32**, 2091 (1992).

DIII-D Results: J.T. Scoville, R.J. La Haye, A.G. Kellmann, T.H. Osbourne, R.D. Stambaugh, E.J. Strait, and T.S. Taylor, Nucl. Fusion **31**, 875 (1991).

JET Results: G.M. Fishpool, and P.S. Haynes, Nucl. Fusion **34**, 109 (1994).